Group-theoretical approach to final-state angular correlations in double photoionization of helium

Yanghui Qiu and Joachim Burgdörfer*
Department of Physics, University of Tennessee, Knoxville, Tennessee 37996-1200
and Oak Ridge National Laboratory, Oak Ridge, Tennessee 37831-6377
(Received 22 April 1998; revised manuscript received 24 November 1998)

We extend the well-known O(4) group-theoretical method for the classification of doubly excited states to the two-electron continuum. The analytical continuation of the approximate dynamic symmetry group across the double ionization threshold is isomorphic to the homogeneous Lorentz group O(3,1). The infinite-dimensional irreducible representations of O(3,1) provide approximate wave functions, which incorporate electron-electron angular correlations. Moreover, the labels of the representations can be interpreted as approximate quantum numbers, which allow the extension of well-known propensity rules from double excitation to double ionization. Employing the *dynamic* O(3,1) symmetry group and a new method to calculate *complex* Wigner $(9\text{-}j)$ coefficients, we determine the angular distributions of the photoelectrons for double photoionization of helium near threshold. We find remarkable agreement with recent measurements. Similarities to and differences from other calculations are discussed. [S1050-2947(99)00204-8]

PACS number(s): 32.80.Fb, 31.15.Ja, 31.25.−v

I. INTRODUCTION

The understanding of correlation effects arising in the dynamics of two electrons escaping from a charged core is of fundamental importance in atomic and few-body physics. Much attention has been given to the double ionization of He and H^- by a single photon because this process occurs only through the effects of correlation. At photon energies near the double-ionization threshold, the studies have focused on the angular and energy distribution of the escaping electrons and on the energy dependence of the total cross section. One milestone of these studies was the Wannier-Rau-Peterkop (WRP) theory [1–3] that predicted that the total cross section for double photoionization of an atom varies above threshold as $\sigma^{++}\propto E^m$, where E is the energy shared by the two photoelectrons and m is an exponent depending on the charge Z of the residual ion. The theoretical values $m=1.127$ for $Z=1$ and $m=1.056$ for $Z=2$ are consistent with experiments for H^- and K^- targets [4,5] and for He [6–9]. Moreover, the WRP theory predicts a strong angular correlation between the escaping electrons with preferred back-to-back emission near threshold. Several theoretical methods have been developed to investigate angular correlations in double ionization [10–15]. While the region close to threshold ($\lesssim$ eV) is still difficult to access by fully numerical *ab initio* treatments, close agreement with experimental data at higher energies has been achieved [15–19].

In the following paper we present an alternative approach to electron-electron angular correlation, which is solely based on the existence of an approximate dynamical symmetry group of the problem. Within this framework, angular correlations follow ''automatically'' from the proper choice of irreducible representations of the final state rather than from the explicit evaluation of transition matrix elements. This resembles threshold laws within which the asymptotic properties in the $E\rightarrow 0$ limit (E, excess energy above the breakup threshold) is independent of the pathway with which the final state is accessed, provided the processes access the same sector of final states characterized by the same exact quantum numbers, for example, $^1S\rightarrow{}^1P$ transitions in photoionization. Similar to the WRP theory, such an approach can provide information about the energy and angular dynamics but not about the absolute cross section. We show in the following that by solely exploiting the approximate dynamical symmetry, the angular correlation pattern for two-electron emission near threshold can be determined without any explicit calculation of the transition operator and without any adjustable parameter.

II. ANALYTIC CONTINUATION OF O(4)

The starting point of our analysis is the well-known approximate O(4) symmetry of doubly excited resonances [20–23]. The dynamical symmetry group belongs to the group chain

$$\mathrm{O}(3)\subset\mathrm{O}(4)\subset\mathrm{O}(4)\times\mathrm{O}(4), \tag{1}$$

where $\mathrm{O}(4)\times\mathrm{O}(4)$ is the product group of hydrogenic electrons with quantum numbers (or labels of the irreducible representations) $n_{1,2},\ell_{1,2},m_{1,2}$ while O(3) is the exact geometric symmetry group with quantum numbers LM. The labels of the irreducible representations of the dynamical O(4) group, K and T, are approximate collective quantum numbers describing bending vibrations and the projection of the angular momentum along the interelectronic axis. Using scaled coordinates $r_i=\tilde{r}_i/Z$, $p_i=\tilde{p}_iZ$, it is seen from the scaled Hamiltonian,

*Present address: Institute for Theoretical Physics, Vienna University of Technology, A-1040 Vienna, Austria.

$$\tilde{H}=-\frac{1}{2}(\tilde{\nabla}_1^2+\tilde{\nabla}_2^2)-\frac{1}{\tilde{r}_i}-\frac{1}{\tilde{r}_2}+\lambda\frac{1}{\tilde{r}_{12}}, \tag{2}$$

with $\lambda=1/Z$, that in the limit of $\lambda\to 0$ ($Z\to\infty$) the symmetry group chain [Eq. (1)] becomes exact. For helium ($\lambda=0.5$) it has been shown [20–28] that the supermultiplet structure, propensity rules, and the angular correlation pattern of doubly excited states are well described by the approximate dynamic O(4) group. Here, we extend the approximate dynamical symmetry group to doubly excited states across the double-ionization threshold based on analytical continuity and obtain an approximate dynamic O(3,1) group symmetry for the double continuum states. Based on the O(3,1) representation of the two-electron wave functions, we investigate the triply differential cross section (TDCS) of He, which can be evaluated from the flux of the final-state wave function ψ_f with the proper boundary conditions [11,27,28], i.e.,

$$\frac{d^3\sigma}{d\Omega_1 d\Omega_2 dE_1}\propto|\psi_f|^2|_{r_i\to\infty\ (i=1,2)}, \tag{3}$$

where $\Omega_{1,2}$ are the solid angles of the emitted electrons and E_1 is the energy of one of the electrons. For a hydrogenic atom, the electron moves in a central field $-Z/r$. The angular momentum $\boldsymbol{l}=\boldsymbol{r}\times\boldsymbol{p}$ and the Runge-Lenz vector $\boldsymbol{a}=(\boldsymbol{p}\times\boldsymbol{l}-Z\hat{\boldsymbol{r}})/\sqrt{2|E|}$ are constants of motion, where $\boldsymbol{p}$ is the momentum of the electron and E the energy. The angular momentum $\boldsymbol{l}$ is perpendicular to the orbit, and the Runge-Lenz vector $\boldsymbol{a}$ is in the plane of the orbit and pointing from the nucleus toward the perigee. When the electron is in a bound state, the orbit is elliptic while for the electrons in the continuum state, the orbit becomes hyperbolic. The angular momentum and the Runge-Lenz vector form Lie algebras with the following commutation rules [29,30]:

$$[l_i,l_j]=i\epsilon_{i,j,k}l_k, \tag{4}$$

$$[l_i,a_j]=i\epsilon_{i,j,k}a_k, \tag{5}$$

$$[a_i,a_j]=\pm i\epsilon_{i,j,k}l_k;, \tag{6}$$

where the + (−) sign refers to negative (positive) one-electron energies. Equations (4)–(6) correspond to the infinitesimal generators of the O(4) (for the + sign) and the O(3,1) symmetry group (for the − sign). The analytic continuation of O(4) across the threshold is therefore O(3,1).

For two-electron atomic systems, the electron-electron interaction leads to the mixing of the degenerate hydrogenic manifolds. The average Coulomb repulsion of the electrons is determined by the relative orientation of the orbits. For pairs of degenerate orbits with total angular momentum $\boldsymbol{L}=\boldsymbol{l}_1+\boldsymbol{l}_2$, the simplest measure of this orientation is the scalar $B^2=(\boldsymbol{a}_2-\boldsymbol{a}_1)^2$. Orbits directed toward opposite sides (larger B^2) of the nucleus repel each other less than two orbits on the same side (smaller B^2) of the nucleus. The simultaneous diagonalization of the commuting operators B^2,L^2,S^2 (total spin), and total parity π for doubly excited states in a subspace of degenerate two-electron hydrogenic configurations yields approximate mixing coefficients induced by the perturbation $1/r_{12}$, i.e., B^2 and $1/r_{12}$ commute with each other approximately. Moreover, B^2 can be represented as a function of generators of the dynamic Lie algebras $O(4)_1$ and $O(4)_2$ of electrons 1 and 2 for hydrogenic orbits. Diagonalization of B^2 is obtained naturally in the irreducible representations of the O(4) group. The labels of the irreducible representation are the quantum numbers of the doubly excited state basis (DESB),

$$|NnKTLM_L\pi\rangle=\sum_{l_1,l_2}|Nl_1nl_2LM_L\pi\rangle D^{KTL\pi}_{Nl_1nl_2}, \tag{7}$$

where M_L is the z component of $\boldsymbol{L}$, l_i ($i=1,2$) are the usual hydrogenic angular-momentum quantum numbers, N and n are the principal quantum numbers of the inner and outer electrons, respectively. Since N and n are assumed to be approximate quantum numbers, radial correlations are neglected. The sum in Eq. (4) is over all values of l_1 and l_2 compatible with a given L and π. The D mixing coefficient is obtained in terms of Wigner $(9\text{-}j)$ symbols as [20–22]

$$\begin{aligned}D^{KTL\pi}_{Nl_1nl_2}=&(-1)^{l_2}[(P+T+1)(P-T+1)\\&\times(2l_1+1)(2l_2+1)]^{1/2}\\&\times\begin{Bmatrix}\frac{(N-1)}{2}&\frac{(n-1)}{2}&\frac{(P+Q)}{2}\\ \frac{(N-1)}{2}&\frac{(n-1)}{2}&\frac{(P-Q)}{2}\\ l_1&l_2&L\end{Bmatrix}\frac{1+(-1)^{T+S}\pi}{\sqrt{2(1+\delta_{T,0})}},\end{aligned} \tag{8}$$

where $P=n-1+K$ and K and T ($=|Q|$) are the DESB quantum numbers. The range of values for (K,T) follows directly from the triangle inequalities incorporated in the $9\text{-}j$ symbol. The energetically most favored state that minimizes the electron-electron repulsion among the doubly excited states for given N,n,L is the state with the maximum positive K value and with the minimum $|T|$ value that also satisfies $\pi(-1)^{T+S}=1$ [28,26], specifically, for fixed $L=1$, $S=0$, the most favored state has quantum numbers $K=N-2$ and $T=1$. The DESB functions incorporate most of the angular correlations. The corresponding appropriate quantum numbers, therefore, permit us to formulate propensity rules for excitation processes, which reflect the conservation of intrinsic few-body correlations.

The idea is now to preserve these salient features for two-electron continuum states by an analytic continuation of the dynamic symmetry group O(4) across the double-ionization threshold. As a result, we obtain the dynamic O(3,1) group for the double continuum states. As a noncompact group, the homogeneous Lorentz group possesses infinite-dimensional irreducible representations. The labels of the infinite-dimensional irreducible representation of the principal series for the O(3,1) group are η_1, η_2, L, η_k, T, and π, where η_1,

η_2, and η_k take continuous values [30–34]. These labels can be directly mapped from the O(4) group onto the O(3,1) group as follows:

$$N \to i\eta_1, \quad L \to L,$$
$$n \to i\eta_2, \quad T \to T,$$
$$K \to i\eta_K, \quad \pi \to \pi, \tag{9}$$

where η_i $(i=1,2)$ are related to the single-particle energies as $E_i = Z^2/(2\eta_i^2)$. The irreducible representation of the principal series for the O(3,1) group can be obtained by applying the analytic continuation from double excitation to double ionization:

$$|\eta_1 \eta_2 \eta_k TLM_L \pi\rangle = \sum_{l_1,l_2} |\eta_1 l_1 \eta_2 l_2 LM_L \pi\rangle D^{\eta_k TL\pi}_{\eta_1 l_1 \eta_2 l_2}, \tag{10}$$

where

$$D^{\eta_k TL\pi}_{\eta_1 l_1 \eta_2 l_2} = (-1)^{l_2}[(P+T+1)(P-T+1) \times (2l_1+1)(2l_2+1)]^{1/2} \times \begin{Bmatrix} \frac{(i\eta_1-1)}{2} & \frac{(i\eta_2-1)}{2} & \frac{(P+T)}{2} \\ \frac{(i\eta_1-1)}{2} & \frac{(i\eta_2-1)}{2} & \frac{(P-T)}{2} \\ l_1 & l_2 & L \end{Bmatrix} \times \frac{1+(-1)^{T+S}\pi}{\sqrt{2(1+\delta_{T,0})}} \tag{11}$$

and $P = i\eta_2 - 1 + i\eta_K$. Note that the O(3,1) mixing coefficient D is now a function of complex argument. The infinite-dimensional irreducible representations provide approximate wave functions for double continuum states ψ_f, which incorporate electron-electron angular correlation. B^2 is also approximately conserved for the double continuum states. The asymptotic form of the double continuum wave function entering Eq. (3) is

$$\psi_f(\mathbf{r}_1,\mathbf{r}_2)|_{r_i\to\infty} = \frac{e^{i(k_1 r_1 + k_2 r_2)}}{r_1 r_2} \sum_{l_1 l_2} D^{\eta_k TL\pi}_{\eta_1 l_1 \eta_2 l_2} \sum_{m_1 m_2} Y_{l_1 m_1}(\hat{\mathbf{r}}_1) \times Y_{l_2 m_2}(\hat{\mathbf{r}}_2) \langle l_1 m_1 l_2 m_2 | LM_L\rangle. \tag{12}$$

Consequently, we obtain

$$\frac{d^3\sigma}{d\Omega_1 d\Omega_2 dE_1} \propto \left| \sum_{l_1 l_2}^{l_{\max}} D^{\eta_k TL\pi}_{\eta_1 l_1 \eta_2 l_2} \sum_{m_1 m_2} Y_{l_1 m_1}(\hat{\mathbf{r}}_1) Y_{l_2 m_2}(\hat{\mathbf{r}}_2) \times \langle l_1 m_1 l_2 m_2 | LM_L\rangle \right|^2. \tag{13}$$

For doubly excited states, $l_{\max}$ in the sum over l_1, l_2 for given L and π is constrained by the principal quantum number N $(l_i \leq N, n)$ while the single particle l distribution in the correlated wave-function peaks near $l_0 \approx \sqrt{N}$ [26]. Analogously, we take $l_{\max} \approx 1/\sqrt{\max(E_1,E_2)}$ for the double continuum state. We note, however, that $l_{\max}$ will be automatically determined when the transition amplitude is explicitly evaluated using ψ_f. We note that Eq. (13) contains the well-known selection rules [35], which originate from the geometric quantum numbers of O(3) (including parity and spin). Moreover, it contains the approximate dynamical propensity rules based on the symmetry group O(3,1).

The implication of Eq. (13) is that the angular distribution and angular correlation pattern can be determined with group-theoretical methods without an explicit evaluation of the transition matrix element. The key input to Eq. (13) is the calculation of complex Wigner $(9\text{-}j)$ coefficients. Extensive studies of the *complex* angular momentum coupling have been performed in the 1960s. Two methods developed by Dolginov and Toptygin [31] and by Anderson *et al.* [32,33] were specifically devoted to the calculation of the *complex* Wigner coefficients. However, we found the method suggested by Dolginov and Toptygin to be impractical to implement while the formulas derived by Anderson *et al.* do not obviously preserve analytical continuity across the threshold. Our method uses recursion relations that hold for real $9\text{-}j$ symbols and which permit analytic continuation. Since we need in the following $(9\text{-}j)$ symbols with $L=1$ and $T=1$, we consider for simplicity,

$$X(N,l_1;n,l_2;Q,T=1,L=1) = (-1)^{l_2}[(2l_1+1)(2l_2+1) \times (P+2)P]^{1/2} D^{K11\pi}_{Nl_1 nl_2}$$

with $Q = n + K$.

After some tedious algebra starting from the commutation rules in Eqs. (4)–(6), we arrive at the recursive relations

$$X(N,1;n,0;Q,1,1) = -\left(\frac{n^2-1}{N^2-1}\right)^{1/2} X(N,0;n,1;Q,1,1), \tag{14}$$

$$X(N,1;n,1;Q,1,1) = \left(\frac{3}{2}\right)^{1/2} \frac{Q}{(N^2-1)^{1/2}} X(N,0;n,1;Q,1,1), \tag{15}$$

$$2\left\{[n^2-(l+1)^2]\frac{l(l+1)}{(2l+1)}\right\}^{1/2} X(N,l;n,l+1;Q,1,1) = -(l+1)^{1/2} Q X(N,l;n,l;Q,1,1) + [(N^2-l^2)(2l+1)]^{1/2} X(N,l-1;n,l;Q,1,1) - \left(\frac{n^2-l^2}{2l+1}\right)^{1/2} X(N,l;n,l-1;Q,1,1), \tag{16}$$

$$2\left\{[N^2-(l+1)^2]\frac{l(l+1)}{(2l+1)}\right\}^{1/2} X(N,l+1;n,l;Q,1,1) = (l+1)^{1/2} Q X(N,l;n,l;Q,1,1) + [(n^2-l^2)(2l+1)]^{1/2} \times X(N,l;n,l-1;Q,1,1) - \left(\frac{N^2-l^2}{2l+1}\right)^{1/2} \times X(N,l-1;n,l;Q,1,1), \tag{17}$$

$$\{[N^2-(l+1)^2]2(l+2)\}^{1/2}X(N,l+1;n,l+1;Q,1,1)$$
$$=[2(2l+3)]^{1/2}QX(N,l;n,l+1;Q,1,1)$$
$$+\left\{[n^2-(l+1)^2]\frac{2l(2l+3)}{(2l+1)}\right\}^{1/2}X(N,l;n,l;Q,1,1). \quad (18)$$

It is easy to show that Eqs. (13)–(17) give the same values of X for real $9j$ symbols as the direct calculation in terms of the $3j$ expansion. With the replacement of $N\rightarrow i\eta_1$, $n\rightarrow i\eta_2$, and $Q\rightarrow i\eta$, the recursion relations yield the corresponding values of the *complex* 9-j symbols. Moreover, since the recursion relations coincide at threshold for both bound states ($n\rightarrow\infty$, $N\rightarrow\infty$) and double continuum states ($\eta_1\rightarrow\infty$, $\eta_2\rightarrow\infty$), the analytic continuity is explicitly preserved. For doubly excited states, the O(4) angular correlation pattern is approximately valid for $n\gg 1$. In turn, by analytic continuation, the range of validity in the continuum is expected to be limited to $\eta_i\gg 1$, i.e., in the near-threshold region for three-body breakup.

III. ANGULAR CORRELATION IN PHOTOIONIZATION

The characterization of the two-electron continuum state in terms of the O(3,1) state labels allows now the straightforward extension of the propensity rules for continuum final states for a given process. We consider in the following double photoionization of helium, where the two electrons are excited from the ground state (^1S) to a doubly-ionized state (^1P) after receiving all of the photon energy and one unit of angular momentum. At this point, we can make explicit use of the fact that the same quantum numbers that describe the collective motion in doubly excited states can also describe the internal motion of continuum states. Specifically, the propensity rules well known for resonances can be extended to the continuum. Accordingly, as for doubly excited states, the most favored ^1P double continuum state for a given η_1, η_2, is the state with $T=1$ and $\eta_K=\eta_1+2i$. The propensity of $T=1$ states has been recently directly demonstrated in multidifferential measurements by Dörner *et al.* [36]. Therefore, we can evaluate the TDCS for double photoionization in Eq. (11) with $L=1$, $S=0$, $T=1$, and $\eta_K=\eta_1+2i$. Near threshold, we have $E_i\rightarrow 0$, $\eta_1\gg 1$, and $\eta_K\approx\eta_1$.

The angular correlation between the two electrons is described by the interelectronic angle Θ_{12} and is in the following displayed for the specific geometry with one electron emitted along the direction of photon polarization. At threshold ($E_1=E_2\approx 0^+$), the two electrons move in (near) opposite directions (Fig. 1), which is in agreement with the WRP theory. Note that the observed angular correlation also closely corresponds to the one observed for doubly excited states. For $K=K_{\max}$, the two electrons are localized predominantly on opposite sides of the nucleus and moved radially out of phase or in phase corresponding to an (anti) symmetric stretch mode. Unlike quasibound resonances, however, for double ionization the in-phase symmetric stretch mode is essential for the escape near threshold.

The O(3,1) description yields the threshold exponent for the $Z\rightarrow\infty$ limit, i.e., $m=1$ that is close to but not identical to the correct exponent for $Z=2$ ($m=1.056$). The differential energy distribution is uniform over the interval $0\leqslant E_1\leqslant E$ in reasonable agreement with classical [37] and *ab initio* quantum calculations [16] that show an almost uniform distribution with a slight dip of the differential cross section near the end point ($E_1\approx 0$) by a few percent. These deviations reflect the fact that the approximate two-electron states neglect radial correlations. Angular correlations, on the other hand, are expected to be more accurately represented. For the limit $E\rightarrow 0^+$, the angular distribution can also be derived from the O(4) group representation for photon energy just below the Wannier threshold ($E_1=E_2=0^-$) invoking the continuity across the double ionization limit.

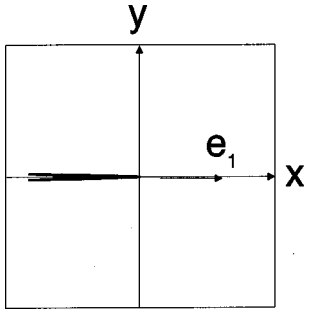

FIG. 1. TDCS for double photoionization of helium. The TDCS is plotted in polar coordinates with respect to the angle θ_2, the emission direction of the second electron with energy E_2 while the emission direction of the first electron with energy E_1 is fixed along the polarization vector $\hat{x}$ of the photon, i.e., $\theta_{12}=\theta_2$. Equal energy sharing with $E_1=E_2=10^{-6}$ eV.

As the electron energies increase, the angular distribution depends on the shared total energy and the partition of the energy. For given total energy $E=0.2$ eV with equal energy sharing $E_1=E_2=0.1$ eV [Fig. 2(a)], the maximum TDCS appears at an angle $\theta_{12}\approx 154°$. For equal energy sharing ($E_1=E_2$), the cross section vanishes at $\theta_2=\theta_{12}=180°$, giving rise to a ''cusp'' in the TDCS. This is due to the fact that for a total angular momentum $L=1$, $\psi_f(\vec{r},-\vec{r})=0$ [see Eq. (12)]. The peak position of the TDCS as a function of Θ_{12} provides a simple measure for the distribution. For unequal energy sharing $E_1=0.2$ eV and $E_2=0^+$ eV [Fig. 2(b)], the peak in the TDCS is at $\theta_{12}\approx 161°$, which is 7° larger than that of equal energy sharing. For unequal energy sharing $E_1=0^+$ eV and $E_2=0.2$ eV [Fig. 2(c)], the maximum of the TDCS is located at $\theta_{12}=180°$. The angular distribution in the extremely asymmetric energy sharing is significantly different from that for the equal energy sharing for fixed total energy E. When $E_1\neq E_2$, a finite value of TDCS at $\theta_2=\pi$ is possible. This gives rise to either a butterfly-shaped distribution for the *correlated* emission of the slower electron or a single-lobe distribution at $\theta=\pi$ for the faster electron. There are no experimental data available for comparison for such low energies, possibly due to the difficulties in detecting low electron energies.

At somewhat higher energies, a comparison with experiment and *ab initio* quantum calculations is possible. In Fig. 3 we show our results along with two different theoretical results of Pont *et al.* [15] and the measurements of Lablanquie *et al.* [7] at $E=4$ eV. The different plots have been rescaled so that the TDCS has the same value at its maximum for all

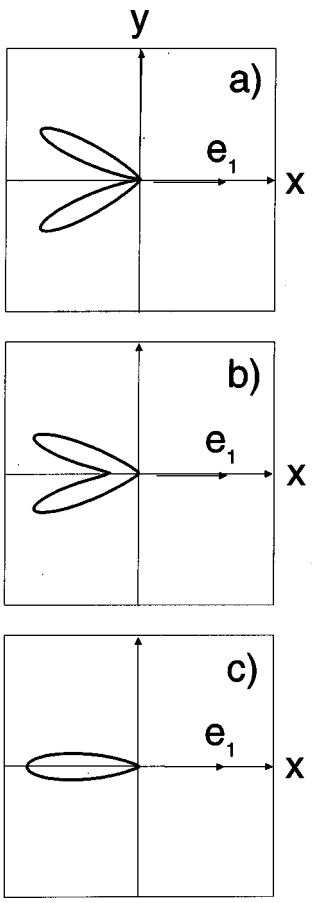

FIG. 2. As Fig. 1 but for energies, (a) $E_1=E_2=0.1$ eV; (b) $E_1=0.2$ eV, $E_2=10^{-6}$ eV; (c) $E_1=10^{-6}$ eV, $E_2=0.2$ eV.

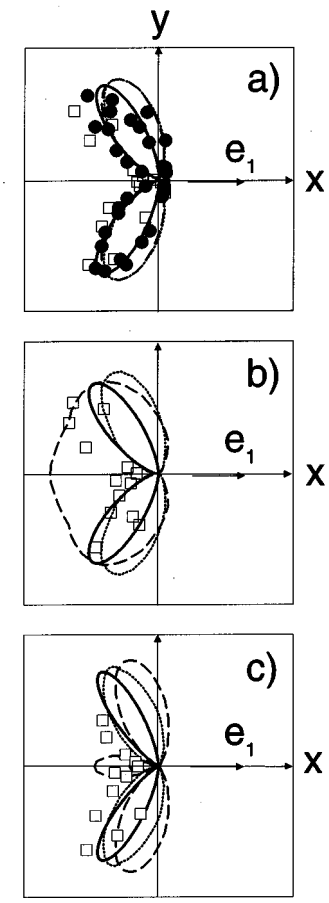

FIG. 3. Comparison between experimental and theoretical angular distributions at $E=4$ eV and different energy partitions: (a) $E_1=E_2=2$ eV; (b) $E_1=3.3$ eV, $E_2=0.7$ eV; (c) $E_1=0.7$ eV, $E_2=3.3$ eV. Open squares, experimental data from Lablanquie *et al.* [7]; solid circles, experimental data from Huetz *et al.* [38]; full curves, current group-theoretical results; dashed and dotted curves, velocity gauge results of 3C theory and 2SC theory from Pont *et al.* [15]. The TDCS is plotted in polar coordinates with respect to the angle θ_2 of the second electron with energy E_2 while the first electron with energy E_1 is emitted along the polarization axis.

sets of data for a given case. For equal energy sharing, $E_1=E_2=2$ eV [Fig. 3(a)], the peak in the TDCS is at $\theta_{12}\approx 122°$. For unequal energy sharing, $E_1=3.3$ eV and $E_2=0.7$ eV [Fig. 3(b)], the maximum of the TDCS can be found at $\theta_{12}\approx 127°$. For the case $E_1=0.7$ eV and $E_2=3.3$ eV [Fig. 3(c)], the maximum of the TDCS appears at $\theta_{12}=122°$. The differences between the angles of the peak position are now smaller but still noticeable. Note that our TDCS are exactly zero at $\theta_{12}=180°$ for equal energy sharing. This node is the direct consequence of the exact symmetry of the ^1P state [35]. The peak position of the distribution, however, is governed by the approximate *dynamic* O(3,1) symmetry group.

The O(3,1) for the angular distribution lies ''in between'' the experimental data and the *ab initio* 2SC calculation of Pont *et al.* [15] and is in somewhat closer agreement with the data. We have shown both the original experimental data of Ref. [7] as well as the corrected data for equal-energy sharing [Fig. 3(a)] [38]. The agreement is significantly improved for the revised data. We emphasize that our present results contain no adjustable parameter and yield comparable, if not better, agreement as a fully numerical state-of-the-art calculation such as the 2SC approach. There are substantial discrepancies between the 2SC results and the approximate 3C results in the same gauge. The experimental peak positions in the angular distribution are approximately equal for equal and unequal energy sharing [7] in agreement with the O(3,1) prediction. Note that the data of Lablanquie *et al.* are not symmetric with respect to the polarization direction. Since retardation effects are expected to be negligible at such low energies and, hence, the angular distribution should be symmetric with respect to the polarization direction, the difference of the peak position in the angular distributions on both sides of the polarization axis can be regarded as a lower bound for the experimental errors, which are about 11° in Figs. 3(a)–3(c). We note that there are now more data available for other geometries [39] for which further tests will become possible in the near future.

In conclusion, we have proposed the analytic continuation of the approximate O(4) dynamical symmetry across the double-ionization limit in terms of the O(3,1) group, the homogeneous Lorentz group. The group-theoretical approach to angular correlations in the continuum provides direct insights into the emission pattern in double ionization. The angular distribution near threshold can be well described based on the approximate dynamical symmetry of the two-electron system without an explicit calculation of the

photoionization. Quantum numbers characterizing propensity rules for excitation processes can be extended across the double-ionization threshold. The difference Runge-Lenz vector B play the role of a collective variable, which contains the emission pattern subject to the constraints of the geometric O(3) quantum numbers.

ACKNOWLEDGMENTS

This work was supported by the NSF and by the U.S. DOE, Office of BES, Division of Chemical Science, under Contract No. DE-AC05-96OR22646 with the Lockheed Martin Energy Research Corporation.

[1] G. H. Wannier, Phys. Rev. **90**, 817 (1953).
[2] A. R. P. Rau, Phys. Rev. A **4**, 207 (1971).
[3] R. Peterkop, J. Phys. B **4**, 513 (1971).
[4] J. B. Donahue, P. A. M. Gram, M. V. Hynes, R. W. Hamm, C. A. Frost, H. C. Bryant, K. B. Butterfield, D. A. Clark, and W. W. Smith, Phys. Rev. Lett. **48**, 1538 (1982).
[5] Y. K. Bae and J. R. Peterson, Phys. Rev. A **37**, 3254 (1988).
[6] R. I. Hall, A. G. McConkey, L. Avaldi, K. Ellis, M. A. M. A. Macdonald, G. Dawber, and G. C. King, J. Phys. B **25**, 1195 (1992).
[7] P. Lablanquie, J. Mazeau, L. Andric, P. Selles, and A. Huetz, Phys. Rev. Lett. **74**, 2192 (1995).
[8] H. Kossmann, V. Schmidt, and T. Andersen, Phys. Rev. Lett. **60**, 1266 (1988).
[9] G. C. King, M. Zubek, P. M. Rutter, F. H. Read, A. A. MacDowell, J. B. West, and D. M. P. Holland, J. Phys. B **21**, L403 (1988).
[10] H. L. Rouzo and C. D. Cappello, Phys. Rev. A **43**, 318 (1991).
[11] A. Huetz, P. Selles, D. Waymel, and J. Mazeau, J. Phys. B **24**, 1917 (1991).
[12] F. Maulbetsch and J. S. Briggs, J. Phys. B **26**, 1679 (1993).
[13] F. Maulbetsch and J. S. Briggs, J. Phys. B **26**, L647 (1993).
[14] M. Pont and R. Shakeshaft, Phys. Rev. A **51**, R2676 (1995).
[15] M. Pont, R. Shakeshaft, F. Maulbetsch, and J. S. Briggs, Phys. Rev. A **53**, 3671 (1996).
[16] D. Proulx and R. Shakeshaft, Phys. Rev. A **48**, R875 (1993).
[17] K. W. Meyer, C. H. Greene, and B. D. Esry, Phys. Rev. Lett. **78**, 4902 (1997), and references therein.
[18] A. S. Kheifets and I. Bray, Phys. Rev. A **54**, R995 (1996).
[19] Y. Qiu, Y. Z. Teng, J. Burgdörfer, and Y. Wang, Phys. Rev. A **57**, R1489 (1998); J. Z. Tang and J. Burgdörfer, J. Phys. B **30**, L523 (1997).
[20] C. E. Wulfman, in *Group Theory and its Application*, edited by E. M. Loebl (Academic, New York, 1971).
[21] D. R. Herrick, Phys. Rev. A **12**, 413 (1975).
[22] D. R. Herrick, M. E. Kellman, and R. D. Poliak, Phys. Rev. A **22**, 1517 (1980).
[23] M. E. Kellman, Phys. Rev. Lett. **73**, 2543 (1994).
[24] D. R. Herrick and O. Sinanŏglu, Phys. Rev. A **11**, 97 (1975).
[25] C. D. Lin, Phys. Rev. A **29**, 1019 (1984).
[26] A. R. P. Rau, Rep. Prog. Phys. **53**, 181 (1990).
[27] R. K. Peterkop, J. Phys. B **16**, L587 (1983).
[28] C. H. Greene, J. Phys. B **20**, L357 (1987).
[29] M. Englefield, *Group Theory and the Coulomb Problem* (Wiley, New York, 1972).
[30] M. Bander and C. Itzykson, Rev. Mod. Phys. **38**, 330 (1966).
[31] A. Z. Dolginov and I. N. Toptygin, Zh. Eksp. Teor. Fiz. **37**, 1441 (1959) [Sov. Phys. JETP **37**, 1022 (1960)].
[32] R. L. Anderson, R. Raczka, M. A. Rashid, and P. Winternitz, J. Math. Phys. **11**, 1050 (1970).
[33] R. L. Anderson, R. Raczka, M. A. Rashid, and P. Winternitz, J. Math. Phys. **11**, 1059 (1970).
[34] M. A. Naimark, *Linear Representations of the Lorentz Group* (Pergamon, London, 1964).
[35] F. Maulbetsch and J. Briggs, J. Phys. B **28**, 551 (1995).
[36] R. Dörner *et al.*, Phys. Rev. Lett. **77**, 1024 (1996); Phys. Rev. A **57**, 1074 (1998).
[37] J. M. Rost, J. Phys. B **27**, 5923 (1994).
[38] A. Huetz, L. Andric, J. Lablanquie, P. Selles, and J. Mazeau, in *The Physics of Electronic and Atomic Collisions*, Proceedings of the XIX International Conference, Whistler, Canada, 1995, edited by L. J. Dube, B. A. Mitchell, W. McConkey, and C. E. Brion, AIP Conf. Proc. No. 360 (AIP, New York, 1995), p. 139.
[39] R. Dörner (private communication).